Appl Phys A (2010) 98: 873–877
DOI 10.1007/s00339-010-5561-z

Applied Physics A
Materials Science & Processing

Light-emitting Si nanostructures formed in silica layers by irradiation with swift heavy ions

G.A. Kachurin · S.G. Cherkova · D.V. Marin · A.G. Cherkov · V.A. Skuratov

Received: 13 October 2009 / Accepted: 6 January 2010 / Published online: 30 January 2010
© Springer-Verlag 2010

Abstract Thin SiO_2 layers were implanted with 140 keV Si ions to a dose of 10^{17} cm^{-2}. The samples were irradiated with 130 Mev Xe ions in the dose range of 3×10^{12}–10^{14} cm^{-2}, either directly after implantation or after pre-annealing to form the embedded Si nanocrystals. In the as-implanted layers HREM revealed after Xe irradiations the 3–4 nm-size dark spots, whose number and size grew with increase in Xe dose. A photoluminescence band at 660–680 nm was observed in the layers with the intensity dependent on the Xe dose. It was found that passivation with hydrogen quenched that band and promoted emission at ∼780 nm, typical of Si nanocrystals. In spectra of pre-annealed layers strong ∼780 nm peak was observed initially. Under Xe bombardment its intensity fell, with subsequent appearance and growth of 660–680 nm band. The obtained results are interpreted as the emission at ∼660–680 nm belonging to the imperfect Si nanocrystals. It is concluded that electronic losses of Xe ions are mainly responsible for formation of new Si nanostructures in ion tracks, whereas elastic losses mainly introduce radiation defects, which quench the luminescence. Changes in the spectra with growth of Xe ion dose are accounted for by the difference in the diameters of Xe ion tracks and their displacement cascades.

G.A. Kachurin (✉) · S.G. Cherkova · D.V. Marin · A.G. Cherkov
Institute of Semiconductor Physics SB RAS, 630090 Novosibirsk, Russia
e-mail: kachurin@isp.nsc.ru
Fax: +7-383-3332771

V.A. Skuratov
Joint Institute for Nuclear Research, 141980 Dubna, Russia

1 Introduction

Studies of Si nanostructures are currently an area of intense investigations. The ongoing drive for smaller Si device dimensions coupled with the discovery of strong luminescence from quantum-sized Si nanocrystals (Si-ncs) [1] stimulates research into the processes of Si nanostructures formation and modification. Si-ncs have been conventionally fabricated by either ion implantation of Si ions into SiO_2 layers or by deposition of SiO_x films followed by annealing. In both cases the optimum conditions have involved a Si excess of about 10–15 at.%, and anneal temperatures above 1000°C. The Si-ncs formed reveal strong luminescence at the wavelengths of 750–850 nm. Along with furnace treatments, the formation of light-emitting Si-ncs employing pulsed annealing with pulse duration of 1 s and less has also proven feasible [2–4]. Pulsed anneals are of high practical importance as they enable one to perform high-temperature heat treatment locally while insignificantly affecting the adjacent regions. This is particularly advantageous for the processing of ultra-large-scale integrated circuits. Irradiation with swift heavy ions (SHI) may be considered, to a certain extent, as a kind of pulse treatment. When SHI penetrate in solid-state targets, their stopping in thin near-surface layers occurs predominantly by electronic (ionization) losses. If the deposited energy density exceeds ∼1 keV/nm, tracks may be forming with the nm-scale diameters, where the carrier concentrations may reach $\sim 10^{22}$ cm^{-3} or even more. The temperature inside the tracks may exceed 5000 K for 10^{-13}–10^{-11} s [5]. The thermal spike model is usually proposed to explain structural transformations under SHI irradiation. Yet, in some cases strong ionization (bond breaking) [6] or Coulomb explosion [7] have to be taken into account. Thus far the processes in SHI tracks are not fully understood.

A few articles related to the bombardment of Si suboxide layers with SHI have been published earlier [8–11]. All the authors used for their studies the deposited SiO_x films with rather high excess Si concentrations. Rodichev et al. [8] observed dark spots of 2–3 nm in diameter after irradiation of monoxide layers with 575 MeV Ni and 863 MeV Pb ions. The spots were attributed to Si nanoclusters, formed in the ion tracks. These authors claimed that the process had not a thermal origin [8]. SiO_x phase separation into Si and SiO_2 was observed under 50 MeV Cu ion irradiation, and it was concluded that the phase separation takes place in the ion tracks in compliance with the process of spinodal decomposition [11]. The presence of Si-ncs was not revealed by Raman spectroscopy even for $x = 0.1$ [11]. On the other hand, the appearance of Si-ncs under irradiation with 100 MeV Ni and 150 MeV Ag ions was detected by the authors of [9] and [10], respectively. However, none of the previous studies revealed the emission at 750–850 nm, typical of Si-ncs.

The aim of the present work is to gain a further insight into the processes of formation and modification of quantum-size Si nanostructures in SiO_2 under SHI bombardment. The study was performed using SiO_2 layers, implanted with Si ions to excess silicon concentrations, optimal for synthesis of light-emitting Si-ncs.

2 Experiment

The samples were formed by implanting Si ions into 0.56 μm thick SiO_2 layers thermally grown on single-crystal Si substrates. The Si ion energy was 140 keV, and the dose was 10^{17} cm^{-2}, providing maximal Si excess of ∼12 at.% at the depth of the mean ion range $R_p \approx 0.21$ μm. Two kinds of the samples were employed for irradiations with 130 Mev Xe ions ($R_p \approx 12$ μm.): those after Si implantation and those subjected to post-implantation annealing at 1100°C for 30 min in N_2 gas to form Si-ncs. The doses of Xe ions ranged from 3×10^{12} to 10^{14} cm^{-2}. The stopping power of the Xe ions in the SiO_2 layers nearly completely (∼99.8%) consisted of electronic losses. Additionally, some samples were passivated by anneals in forming gas (94% Ar + 6% H_2) at 500°C for 1 h. The structural and optical properties were controlled by cross-sectional high resolution electron microscopy (HREM) and by photoluminescence (PL) spectroscopy, excited at room temperature by an argon laser at the wavelength $\lambda = 488$ nm.

3 Results

Figure 1 shows a HREM image of as-implanted SiO_2 layers after Xe ion bombardment to doses of 3×10^{12} and 10^{14} cm^2. One can see that in both cases HREM pictures exhibit 3–4 nm-size dark spots. They were not observed by HREM before SHI irradiation. The surface density of the spots was of the order of 10^{12} cm^{-2}. An increase in the irradiation dose resulted in a growth of number and size of the spots (Fig. 1). In some of them lattice fringes may be distinguished with the interplanar spacing matching those of silicon {111} (not shown).

PL spectra of Si implanted samples before and after Xe bombardment are shown in Fig. 2. In the spectra of the samples a broad band peaking at 660–680 nm was observed. Under irradiation with Xe ions the intensity of the band varied with the dose non-monotonously, maintaining the spectral position of its maximum. Initially the irradiation causes the intensity to decrease, however, further bombardment results in growth of PL with a tendency to saturation at the dose of 10^{14} cm^2 (Fig. 2, inset). A weak shoulder near ∼800 nm was seen as well.

In order to passivate the defects, introduced by Xe irradiation, the samples were subjected to the low-temperature anneals in the forming gas. Such a treatment has led to an unexpected interesting result. Passivation quenched the 660–680 nm PL band, but simultaneously a more intensive PL peak at ∼780 nm appeared (Fig. 3). The dependence of the 780 nm PL intensity on the Xe dose quite differed from that for the 660–680 nm band. After the lowest SHI dose of 3×10^{12} cm^{-2} the highest PL intensity was observed; it was even higher than that before Xe irradiation (Fig. 3). However, further bombardment led to continuous diminishing of the peak with the position in the spectrum being unaffected.

Annealing of the Si implanted samples at 1100°C for 30 min resulted in the appearance of intense PL band at

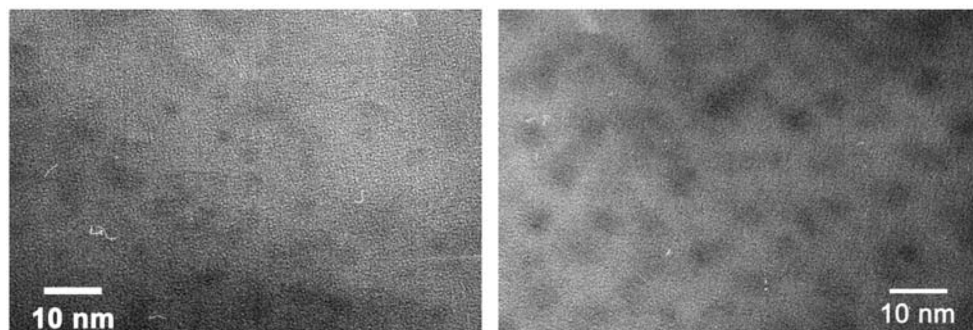

Fig. 1 HREM images of the Si-implanted SiO_2 layers after Xe ion bombardment to the doses of 3×10^{12} (*left*) and 10^{14} cm^2 (*right*)

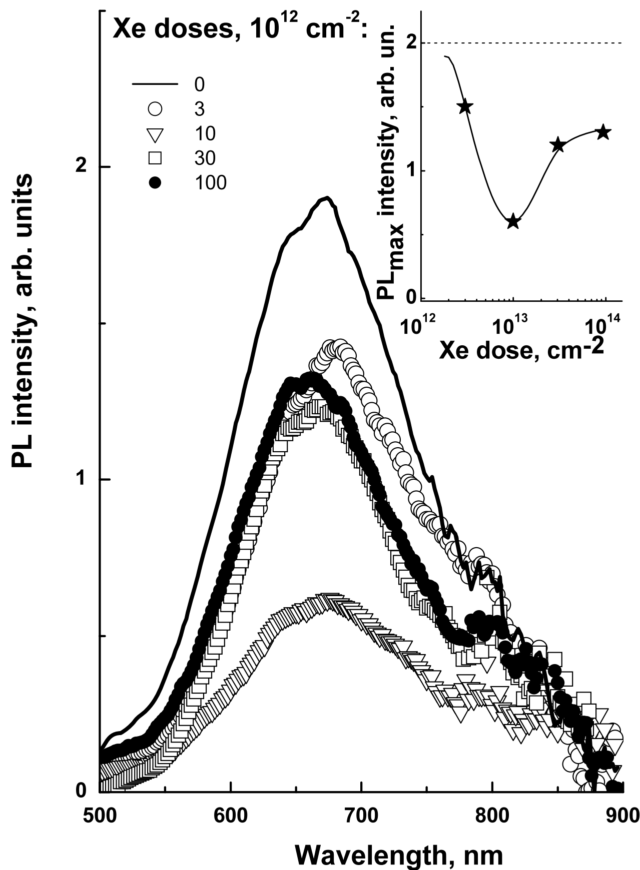

Fig. 2 PL spectra of the Si-implanted SiO_2 layers before and after irradiation with different doses of Xe ions. *Inset*—dependence of 660–680 nm band maximal intensity on the dose of Xe ions, *dashed line*—maximal intensity before SHI irradiation

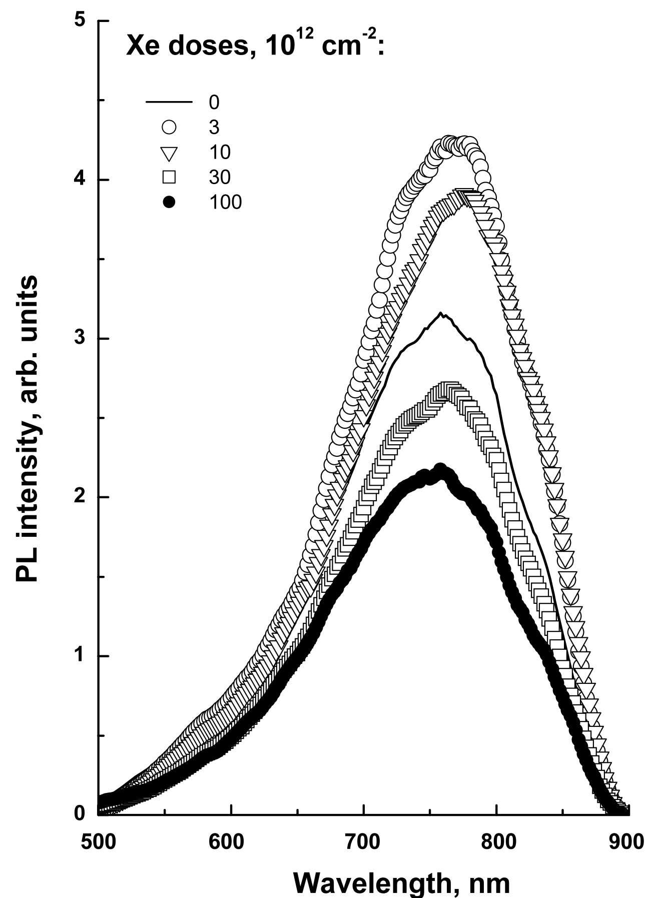

Fig. 3 PL spectra of the Si-implanted SiO_2 layers after Xe ion bombardments followed by hydrogen passivation

~780 nm (Fig. 4). This PL band is well consistent with those usually observed from Si-ncs embedded in SiO_2 matrix. The lowest dose of Xe ions (3×10^{12} cm^{-2}) diminished PL intensity by more than for an order. Further SHI irradiation quenched the 780 nm peak nearly completely, but simultaneously a broad band at about 660–680 nm appeared and rose in intensity with the ion dose (Fig. 4). The PL spectra of Si-ncs, damaged by Xe irradiation, after the passivation were found to be transformed (Fig. 5), akin to the changes observed after passivation of the first set of samples (Figs. 2 and 3). The peak at 660–680 nm was not seen at all and the emission at ~780 nm was found to be restored, however, not completely. For high SHI doses the passivation was less effective, and the spectral distributions of PL intensities looked more flat, as if they consisted of two or more bands between 600 nm and 900 nm (Fig. 5).

4 Discussion

The obtained results point out that irradiation with 130 MeV Xe strongly influences the properties of the nanostructures, being capable to increase number and size of the nanoprecipitates, and to essentially transform PL spectra. Unlike the previous studies [8–11], where the deposited SiO_x layers have been used, our SHI irradiations followed high dose implantation of 140 keV Si ions. To realize the physical mechanisms of the effects observed, one has to compare the nuclear (elastic) and electronic (ionization) energies deposited in the layers by both types of the ions.

According to the SRIM code (www.srim.org), the elastic losses of Xe ions in the oxide layers were only ~0.6 displacement/nm. The elastic energy losses of Si were ~6 displacement/nm, so at the completing stages of implantation (e.g. $<10^{15}$ cm^{-2} is left to implant), when the layers contained nearly full amount of excess silicon, Si ions introduced at least for an order more displacements than Xe. On the other hand, electronic energy losses of Si ions were ~0.2 keV/nm, while for SHI they achieved ~14 keV/nm. Therefore, Si segregation and growth of the nanoprecipitates under Xe ion irradiation (dark spots in Fig. 1) were mainly due to the electronic energy losses of SHI. It should be noted that the elastic losses may also stimulate phase separation in Si-rich SiO_2 [12].

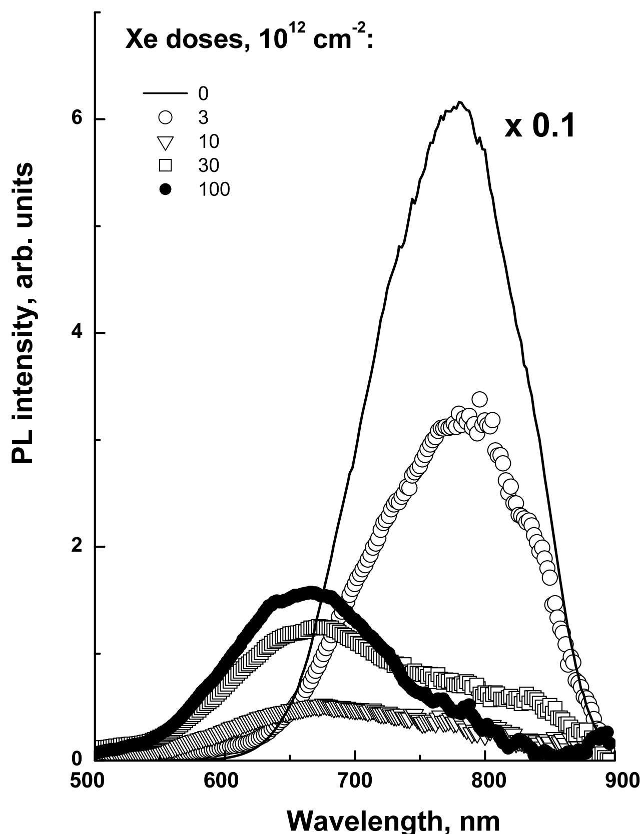

Fig. 4 PL spectra of the layers with embedded Si-ncs before and after irradiation with different doses of Xe ions

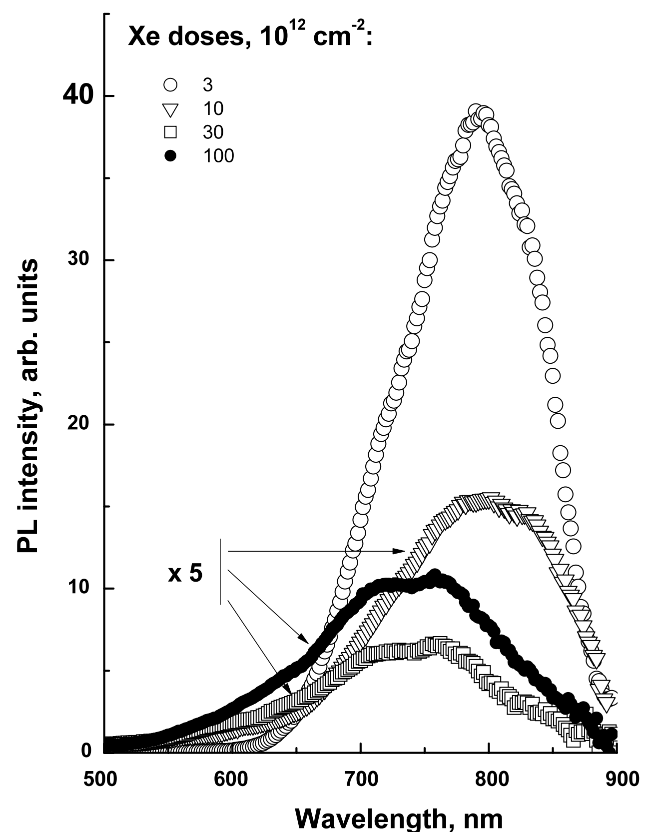

Fig. 5 PL spectra of the layers with embedded Si-ncs after irradiations with Xe ions followed by hydrogen passivation

The indication of crystallization of the nanoprecipitates gives the experiments with passivation (Figs. 2, 3), where the emission at 660–680 nm was substituted by the 780 nm band, widely observed for Si-ncs embedded in SiO_2 layers (for example, typical emission spectrum of Si-ncs see in Fig. 4, solid line). Earlier, PL bands between 500 nm and 700 nm were observed in the cases where either the annealing temperature and time, or the concentrations of excess Si were insufficient for the formation of perfect Si-ncs [13–16]. Such PL bands were attributed to a lot of different Si nanoprecipitates. The position of PL maximum in [13–16] was slightly varying, that was supposed to be due to the differences in size, structure or shape of the precipitates. Our results of passivation may be interpreted as a healing of damaged Si-ncs. Heating up to 500°C while having passivation could not, by itself, lead to crystallization. One can speculate that PL at ~780 nm results from the direct recombination of free excitons in Si-ncs, whereas the PL band at 660–680 nm is due to the recombination of the carriers on the radiative recombination centers created by the structural defects. To the point is that the dark spots were not found by HREM before SHI irradiation, however, a 660–680 nm band was seen immediately after Si implantation (Fig. 2). That may be realized as Si nanoprecipitates were too small to be detected by HREM, but they already contained the appropriate recombination centers.

It is seen in Fig. 2 that an increase in Xe dose from 3×10^{12} cm^{-2} to 10^{13} cm^{-2} decreases the PL band at 660–680 nm, but subsequent Xe irradiations increase the emission. The non-monotonous dependence of the PL intensity on Xe dose we explain by a presence of two processes—introduction of radiation defects and growth of new Si nanostructures. The SHI doses needed to cover completely the sample surfaces with tracks or with damaged areas differ from each other, because the diameter of SHI tracks is several nm [5], while that of the displacement cascades for Xe ions is ~50 nm, according to the SRIM code. The irradiated part of a sample surface S is determined by an expression: $S = S_0[1 - \exp(-cQ)]$, were S_0 is the full sample area, c stands for the cross-sections of the tracks and displacements cascades, and Q denotes the Xe ion dose. The sample surface will be completely overlapped with the displacement cascades at a dose of $\sim 3 \times 10^{11}$ cm^{-2}, whereas to overlap it fully with Xe ion tracks the dose should be roughly two orders higher. Therefore, at low doses the contribution of elastic losses dominates and the defects cause the 660–680 nm band to diminish. We think the elastic losses (displacement cascades) are responsible as well for the leap of 780 nm PL intensity seen in Fig. 3 after the low doses. The

effect may be explained by the radiation-induced crystallization, which was observed and discussed earlier [17–19]. The effect was maximal after the lowest Xe dose and further SHI irradiations lead to accumulation of the defects that hampers activation of 780 nm PL by the subsequent hydrogen treatment (Fig. 3).

The results of the experiments on Xe ion irradiation of prefabricated Si-ncs, are in agreement with the idea that the PL peak in the wavelength range of 660–680 nm belongs to the defective Si-ncs. Increasing the Xe ion dose decreased the intensity of Si-ncs PL (∼780 nm) and caused the appearance of PL near ∼660–680 nm (Fig. 4). Subsequent passivation quenches the shortwave emission and restores PL of Si-ncs, at least in part (Fig. 5). It should be noted that the main drop of Si-ncs PL intensity occurred after the minimal dose of Xe ions—3×10^{12} cm^{-2}. Such a dose is sufficient to cover the samples area with the displacement cascades. Having the elastic energy losses of ∼0.6 displacement/nm, Xe ions will introduce into Si-ncs only isolated atomic displacements. According to the experimental data [17, 20] and theoretical predictions [21] even a single defect in a nanocrystal quenches its PL, provided this defect represents a non-radiative recombination center. Thus, elastic losses of SHI may be responsible for the quenching of PL. On the other hand, if we compare the drop of PL intensity after irradiation with SHI and after introduction of the same dpa by the middle energy ions [20], it will be seen that quenching by SHI goes faster. Therefore a contribution of the elastic losses to the structural damage has to be taken into account. It should be mentioned that our highest Xe dose of 10^{14} cm^{-2} displaced only ∼2% atoms in Si-ncs, while the experiments [17, 20] and theoretical calculations [22, 23] show 10–20% of atoms should be displaced to render Si-ncs amorphous (for bulk Si ∼100%). Restoration of Si-ncs-like PL by annealing in forming gas after the dose of 10^{14} cm^{-2} pointed to the partial retaining of crystallinity after all the SHI doses used.

5 Conclusion

Thin thermally grown SiO_2 layers, containing either Si implanted to the concentrations up to ∼12% or preformed embedded Si-ncs, were irradiated with 130 MeV Xe ions to the doses ranging between 3×10^{12} cm^{-2} and 10^{14} cm^{-2}. HREM revealed in the SHI irradiated Si-rich layers the 3–4 nm-size dark spots, whose number and size grew with increase in Xe ion dose. In parallel PL measurements found the band at 660–680 nm, whose intensity changed with the dose of SHI. It is established that passivation with hydrogen quenches the band and leads to the appearance of ∼780 nm emission, characteristic of Si-ncs. Therefore emission at ∼660–680 nm may be ascribed to imperfect Si-ncs. The results obtained on the irradiation of SiO_2 layers with the embedded Si-ncs are in agreement with that assumption. Electronic energy losses of Xe ions are mainly responsible for the growth of Si nanostructures in the SHI tracks, whereas elastic losses of ions introduce defects within their displacement cascades and quench PL. The observed dependence of PL spectra on Xe ion dose is accounted for by the difference in the diameters of the Xe ion tracks and of their displacement cascades.

Acknowledgements We thank Dr. V.V. Kirienko for the anneals in forming gas. This work has been supported by the Grant No. 08-02-00221 (Russian Foundation for Basic Researches).

References

1. H. Takagi, H. Ogawa, Y. Yamazaki, A. Ishizaki, T. Nakagiri, Appl. Phys. Lett. **56**, 2379 (1990)
2. G.A. Kachurin, S.G. Cherkova, D.V. Marin, R.A. Yankov, M. Deutschmann, Nanotechnology **19**, 355305 (2008)
3. G.A. Kachurin, I.E. Tyschenko, W. Skorupa, R.A. Yankov, K.S. Zhuravlev, N.A. Pazdnikov, V.A. Volodin, A.K. Gutakovskii, A.F. Leier, Semiconductors **31**, 626 (1997)
4. G.A. Kachurin, I.E. Tyschenko, K.S. Zhuravlev, N.A. Pazdnikov, V.A. Volodin, A.K. Gutakovskii, A.F. Leier, W. Skorupa, R.A. Yankov, Nucl. Instrum. Methods B **122**, 571 (1997)
5. M. Toulemonde, Ch. Dufour, A. Meftah, E. Paumier, Nucl. Instrum. Methods B **166–167**, 903 (2000)
6. H. Hosono, K. Kawamura, Y. Kameshima, H. Kawazoe, N. Matsunami, K. Muta, J. Appl. Phys. **82**, 4232 (1997)
7. R.L. Fleischer, P.B. Price, R.M. Walker, J. Appl. Phys. **36**, 3645 (1965)
8. D. Rodichev, Ph. Lavallard, E. Dooryhee, A. Slaoui, J. Perriere, M. Gandais, Y. Wang, Nucl. Instrum. Methods B **107**, 259 (1996)
9. P.S. Chaudhari, T.M. Bhave, D. Kanjilal, S.V. Bhoraskar, J. Appl. Phys. **93**(6), 3486 (2003)
10. P.S. Chaudhari, T.M. Bhave, R. Pasricha, F. Singh, D. Kanjilal, S.V. Bhoraskar, Nucl. Instrum. Methods B **239**, 185 (2005)
11. W.M. Arnoldbik, N. Tomozeiu, E.D. van Hattum, R.W. Lof, A.M. Vredenberg, F.H.P.M. Habraken, Phys. Rev. B **71**, 125329 (2005)
12. V.G. Kesler, S.G. Yanovskaya, G.A. Kachurin, A.F. Leier, L.M. Logvinsky, Surf. Interface Anal. **33**, 914 (2002)
13. P. Mutti, G. Ghislotti, S. Bertoni, L. Bonoldi, G.F. Cerofolini, L. Meda, E. Grilli, M. Guzzi, Appl. Phys. Lett. **66**, 851 (1995)
14. G. Ghislotti, B. Nielsen, P. Asoka-Kumar, K.G. Lynn, A. Gambhir, L.F. Di Mauro, C.E. Bottani, J. Appl. Phys. **79**, 8660 (1996)
15. S.P. Withrow, C.W. White, A. Meldrum, J.D. Budai, D.M. Hembree Jr., J.C. Barbour, J. Appl. Phys. **86**, 396 (1999)
16. Y. Batra, T. Mohanty, D. Kanjilal, Nucl. Instrum. Methods B **266**, 3107 (2008)
17. G.A. Kachurin, S.G. Yanovskaya, M.-O. Ruault, A.K. Gutakovskii, K.S. Zhuravlev, O. Kaitasov, H. Bernas, Semiconductors **34**, 965 (2000)
18. M. Klimenkov, W. Matz, S.A. Nepijko, M. Lehman, Nucl. Instrum. Methods B **179**, 209 (2001)
19. X. Du, M. Takeguchi, M. Tanaka, K. Furuya, Appl. Phys. Lett. **82**, 1108 (2003)
20. G.A. Kachurin, S.G. Cherkova, D.V. Marin, A.K. Gutakovsky, A.G. Cherkov, V.A. Volodin, Semiconductors **42**, 1127 (2008)
21. M. Lannoo, C. Delerue, G. Allan, J. Luminescence **70**, 170 (1996)
22. L. Pelaz, L.A. Marques, J. Barbolla, J. Appl. Phys. **96**, 5947 (2004)
23. L.A. Marques, L. Pelaz, J. Hernandez, J. Barbolla, Phys. Rev. B **64**, 045214 (2001)